Fuel 254 (2019) 115569

Contents lists available at ScienceDirect

Fuel

journal homepage: www.elsevier.com/locate/fuel

Full Length Article

Skeletal mechanisms for prediction of NO_x emission in solid fuel combustion

Tian Li[a,*], Øyvind Skreiberg[b], Terese Løvås[a], Peter Glarborg[c]

[a] Department of Energy and Process Engineering, Faculty of Engineering, NTNU — Norwegian University of Science and Technology, Trondheim, Norway
[b] Thermal Energy Department, SINTEF Energy Research, Trondheim, Norway
[c] Combustion and Harmful Emission Control (CHEC) Research Centre, Department of Chemical and Biochemical Engineering, Technical University of Denmark, Lyngby, Denmark

ARTICLE INFO

Keywords:
NO_x
Chemical kinetics
Mechanism reduction
Combustion
Solid fuel
SNCR

ABSTRACT

Emission of nitrogen oxides (NO_x) is a major challenge for combustion of solid fuels. Strategies for emission control can be developed from computational fluid dynamics (CFD) simulation. This, furthermore, requires a computational efficient kinetic model that is able to capture both formation and destruction of NO_x in a wide range of conditions. In this work, three skeletal mechanisms with varying degrees of reduction were developed based on a detailed kinetics model proposed recently (148 species and 2764 reactions). By preserving all major reaction pathways of NO formation, the most comprehensive skeletal mechanism Li45 (45 species and 788 reactions) behaved very similar compared to the base mechanism with regard to the prediction of NO. The more compact skeletal mechanism Li37 (37 species and 303 reactions) was generated specifically for the conditions relevant to large scale industrial combustion of solid fuels. The Li37 mechanism is capable of predicting NO formation as well as simulating common measures of NO_x reduction such as the staged combustion and selective non-catalytic reduction (SNCR). Without the consideration of SNCR, the smallest skeletal mechanism Li32 (32 species and 255 reactions) still maintained a good predictability over broad temperature and excess air ratio ranges. Compared to the base mechanism, the skeletal mechanisms achieved over 70% reduction in species. Furthermore, the computational cost was lowered to a large extent, particularly with Li37 and Li32. This makes the developed skeletal mechanisms very suitable to be implemented in CFD simulations.

1. Introduction

Combustion of solid fuels is a widely used process to provide energy at both industrial and domestic scales. This includes production of energy from renewable sources such as biomass. Combustion of solid fuels is also an effective means to handle municipal solid waste (MSW), since both weight and volume of the MSW can be significantly reduced through incineration. Over the years, various combustion systems have been developed for combustion of solid fuels including grate-firing, suspension-firing, and fluidized-bed furnaces. Owing to the flexibility of accommodating fuels with a wide range of types, sizes, and moisture contents, the grate-firing furnace is the most common technology used for combustion of biomass and MSW, thus also the focus of this study. One drawback of combustion of solid fuels is the emission of nitrogen oxides (NO_x). NO_x may form from fixation of N_2 in air as well as release and transformation of the N-containing organic compounds in solid fuels. Due to the increasingly stringent emission regulations [1], primary or secondary measures, or both, need to be applied to reduce NO_x emission in combustion systems. The primary measures refer to the methods that modify the combustion process such as staged combustion and reburning. The secondary measures, on the other hand, are the means that take place after the combustion chamber, for example, selective non-catalytic reduction (SNCR) and selective catalytic reduction (SCR) by ammonia injection in the flue gas channel at respectively high and low temperature [2]. The secondary measures, being highly effective, is however typically expensive to construct and to operate [3]. As a result, the primary measures have gained rising popularity [4]. In order to maximize the potential of the primary measures, a good understanding of the combustion process is essential. Thus, it is particularly important to improve chemical kinetic models that are able to well capture the formation and consumption of NO_x as well as the combustion of fuels in a wide range of operating conditions.

Kinetic modeling of nitrogen chemistry during combustion has been extensively studied over several decades [5–9]. A recent study by Glarborg et al. [10] comprehensively reviewed this topic, in which primary pathways of NO formation as well as the chemistry of in situ reduction of NO were discussed. A detailed reaction mechanism was also provided together with updated thermodynamic properties, which

* Corresponding author.
E-mail address: tian.li@ntnu.no (T. Li).

https://doi.org/10.1016/j.fuel.2019.05.152
Received 11 March 2019; Received in revised form 21 May 2019; Accepted 28 May 2019
Available online 13 June 2019

were re-evaluated using the Active Thermochemical Tables approach [11,12]. Similar detailed kinetic models have been proposed by other groups e.g., the POLIMI kinetic mechanism, which is able to simulate pyrolysis, partial oxidation, and combustion of hydrocarbon and oxygenated fuels with NO_x formation [13–16]. These comprehensive kinetic models are usually evaluated thoroughly by comparing against experimental data, and are capable of predicting NO_x emission in a broad range. However, they contain a large number of species and nonlinearly coupled reactions and are very expensive to be solved. This makes detailed kinetic models currently too costly to be directly coupled with large-scale computational fluid dynamic (CFD) simulations, which have become the industry standard. Therefore, the complexity of the kinetic models needs to be reduced in order to be useful in such studies.

Decreasing the size of the chemical mechanism is a common practice in order to reduce the computational cost. This is usually done by employing methods such as reaction flow and sensitivity analysis, lumping, and/or time-scale analysis [17,18]. It should be noted that in accordance with the previous study [18], the term *skeletal* mechanism is used in this work to refer to the mechanism that is generated by removing unimportant species and reactions from the detailed mechanism. This should be distinguished from a *reduced* mechanism where the reactions in the original mechanism are lumped or modified by assumptions such as quasi steady state [19]. Very few skeletal mechanisms for modelling of nitrogen chemistry during combustion of solids can be found in the open literatures. Houshfar et al. [20] developed three skeletal mechanisms with 26, 35, and 52 species respectively, based on a detailed kinetic model consisting of 81 species, by employing a reaction flow and sensitivity analysis [21]. It was found that under high-temperature oxidation conditions, all three skeletal mechanisms gave reasonable results, apart from predictions of some minor species. At lower temperatures (less than 1223 K), however, only the skeletal mechanism, whose size was close to the original mechanism, was able to predict NO_x emission within a relatively small tolerance compared to the detailed mechanism. A follow-up investigation by Løvås et al. [22] provided three updated skeletal mechanisms using a combined reaction flow and sensitivity analysis. Among the proposed mechanisms, the 36 species mechanism (denoted as Lovas36) achieved up to 80% reduction in CPU time while at the same time maintaining satisfactory predictabilities in a broad temperature range. Jepsen [23] developed also a skeletal mechanism based on the detailed mechanism from Glarborg et al. [10]. This skeletal mechanism was obtained using the simulation error minimization connectivity method [24] and principal component analysis. The mechanism contains 38 species and 251 reactions (denoted as Jepsen38). It was demonstrated that the skeletal mechanism predicted well the NO formation from the stoichiometric to fuel-rich conditions at temperatures from 1173 to 1673 K. However, it over-estimated the NO formation under fuel-lean conditions.

All the above-mentioned skeletal mechanisms were generated with the emphasis on predicting NO_x emission during combustion processes. However, the applicability of those mechanisms for simulating NO_x reduction by primary or secondary measures is unknown. There are a few skeletal mechanisms [23,25,26] which were proposed dedicated for predicting NO_x reduction. However, to the authors- knowledge, no skeletal mechanisms have been developed to take account of the combustion of volatiles released from solid fuels, the transformation of N-containing organic compounds, and the reduction of NO by means of SNCR at the same time. This study, therefore, aims to identify the important species and reaction pathways in the newly proposed detailed mechanism [10] for predicting NO_x emission during combustion of solid fuels and to propose skeletal mechanisms that are applicable in a wide range of operational conditions. These include environments relevant to two common NO_x reduction technologies, staged-air combustion and SNCR. The investigated conditions cover not only the typical operating envelope for grate-firing furnaces but also the majority of the combustion scenarios in fluidized-bed and suspension-firing furnaces.

This paper is organized as follows. The methodology applied in this study is first outlined, including an overview of the detailed mechanism proposed by Glarborg et al. [10], followed by a concise explanation of the employed automatic reduction technique, an introduction of the reduction procedure, and a detailed description of all the tested conditions. The resulting skeletal mechanism from the preliminary reduction is then presented and validated against multiple experimental results, followed by the introduction and analysis of the two skeletal mechanisms developed from the further reduction of this. The performance and applicability of all three skeletal mechanisms are furthermore investigated for a broad range of conditions relevant for combustion of solid fuels. Concluding remarks are given at the end.

2. Methodology

2.1. Overview of the base mechanism

The skeletal mechanisms were developed from the base mechanism proposed recently by Glarborg et al. [10], which includes detailed submodels for combustion of light hydrocarbons and oxidation of light fuel-nitrogen species. The mechanism contains 148 species and 2764 reactions (1397 reversible reactions), which is denoted as Glarborg148. The original mechanism was slightly modified by removing all the PLOG parameters (pressure dependence rate constants) since only atmospheric combustion was investigated. To be able to predict well the NO_x emission, it is important to identify the important stable species

Table 1
Main conversion pathways and species in NO formation.

Path	NH_3 oxidation	HCN oxidation	HNCO oxidation	Thermal NO	Prompt NO	Formation via N_2O	Formation via NNH
Species	H	CN	HNCO	H	CH	H	H
	HNO	H_2O	N_2	N	CN	N_2	HO_2
	N	HCN	N_2O	N_2	H	N_2O	N_2
	N_2	NHCO	NCO	NO	HCN	NH	N_2O
	N_2O	N_2	NO	O	NH	NO	NH
	NO_2	N_2O	O	O_2	N	O	NNH
	NH	NCO	OH	OH	N_2	O_2	NO
	NH_2	NO			NCN	OH	O
	NH_3	O			NCO		O_2
	NNH	O_2			NO		OH
	NO	OH			O		
	O						
	O_2						
	OH						

and short-lived intermediates involved in the main conversion pathways of N-containing species, which have been detailed in previous studies [5,8,10]. An overview is given in Table 1. It should be noted that only homogeneous NO_x reactions are considered here. NO may also form through heterogeneous reactions during the conversion of char [5].

2.2. Necessity analysis

An automatic reduction method, necessity analysis, was employed in this study. The method was proposed by Soyhan et al. [27], which considers both flow analysis and sensitivity analysis. A necessity index I (relative importance) of a species i is defined as

$$I_i = \max(I_j f_{ij}^a,\ I_j c_{ij}^a,\ I_i; j = 1, N_s,\ a = 1, N_a) \quad (1)$$

where f_{ij}^a and c_{ij}^a are two parameters obtained from the flow analysis describing the flow of atom a between species i and j by formation and consumption, respectively. N_s and N_a are total number of species and atoms, respectively. This equation is solved iteratively, and the initial value is calculated from

$$I_{i,0} = \max\left(\frac{S_{ji}}{\max_{k=1,N_s}(S_{jk})}, \delta_i\right) \quad (2)$$

where S_{ji} and S_{jk} are sensitivities of species j on species i and k, respectively, which are given by the sensitivity analysis, and δ_i is a parameter set by the user. Typically, all the initial reactants and fully reacted products are given a value of 1 for the δ, which implies a high level of importance. Once the necessity index I is evaluated for all the species, a species necessity list can be generated by selecting all the species with an I larger than a preset value. The skeletal mechanisms can therefore be created by eliminating all the redundant species (i.e. the species not in the species necessity list) from the original mechanisms. Detailed information regarding flow analysis and sensitivity analysis can be found in previous works [22,27,28].

2.3. Reduction procedure

The overall reduction procedure is shown in Fig. 1. The preliminary reduction was carried out in two steps. In the first step, a skeletal mechanism was produced based on the necessity analysis ($I \geqslant 0.1$) at 1073 K under atmospheric pressure. An isothermal perfectly stirred reactor was used with a residence time of 1 s. The applied gas composition is listed in Table 2. This condition resembles the environment in the primary zone of a staged biomass combustion reactor [29], which operated with a primary excess air ratio (λ_p) of 0.8. The relatively high nitrogen content released from the solid fuel makes it relevant to waste incineration as well. The same condition has also been used in previous reduction works [20,22]. Since a relative large cutoff limit was applied, the skeletal mechanism produced directly from the necessity analysis may not preserve all main pathways and species listed in Table 1. Therefore all the species, which are listed in Table 1 but not in the skeletal mechanism generated by the necessity analysis, were added together with the related reactions in the second step. By further reduction, more compact mechanisms were developed by a comparative analysis between the skeletal mechanism obtained from the primary reduction and two existing skeletal mechanisms, Lovas36 [22] and Jepsen38 [23]. Details are presented in Section 3.2.

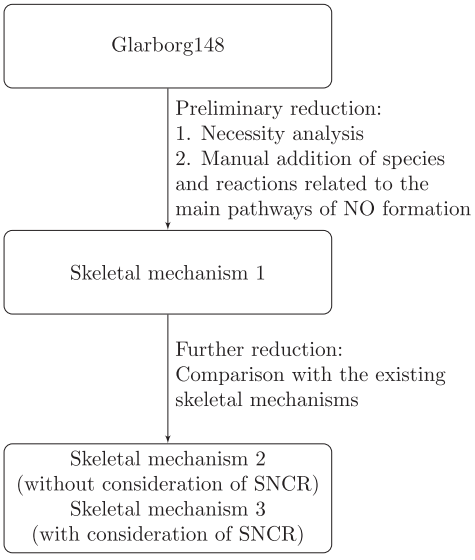

Fig. 1. Overview of the reduction produce.

Table 2
Gas composition considered in the reduction.

Species	Mole fraction	Species	Mole fraction
Ar	0.00698	H_2	0.03447
C_2H_2	0.00056	H_2O	0.08064
C_2H_4	0.00560	HCN	0.00110
C_2H_6	0.00280	N_2	0.58411
CH_4	0.02239	NH_3	0.00169
CO	0.12128	NO	0.00014
CO_2	0.02416	O_2	0.11406

2.4. Validation conditions

Multiple experiments covering the major pathways of NO_x formation were selected to validate the developed skeletal mechanisms. In addition, the predictability of the skeletal mechanisms on SNCR were tested by comparing with the experiments carried out under relevant conditions. This includes three promising technologies: SNCR with NH_3 (Thermal DeNOx) [30], SNCR with cyanuric acid (RapReNOx) [31], and SNCR with urea (NOxout) [32]. It should be noted that due to the lack of well characterized experiments on NO_x emission during combustion of biomass, an experiment on conversion of coal-gasified fuel [33] was also selected. In addition, validation was also carried out by comparisons between the skeletal mechanisms and the base mechanism. Various temperatures, excess air ratios, speciation of NO precursor, and staging configurations were tested in idealized homogenous isothermal reactors covering a broad range of operating conditions. All the tested conditions are listed in Table 3. LOGEresearch [34], a chemical kinetics software, was used to perform all the simulations.

3. Results and discussion

3.1. Preliminary reduction

Table 4 shows the results calculated from the necessity analysis based on the condition described in Table 2. Only the input species and the species with a necessity index larger than 0.1 were preserved in the skeletal mechanism. Compared to the species listed in Table 1, only a few are missing, including HNO, N, N_2O, NH, CN, HNCO, NCO, CH, and NCN. After adding those species and their corresponding reactions, a skeletal mechanism was produced containing 45 species and 788 reactions (394 reversible reactions), which is denoted as Li45. The complete mechanism in CHEMKIN format can be found in the Supplemental material.

Fig. 2 shows the validation of the Li45 mechanism against multiple experimental data described in Table 3. The base mechanism Glarborg148 and the two existing skeletal mechanisms Jepsen38 and Lovas36 were also tested for comparison reasons. The predictions using Li45 are in good agreement with the experiments under all investigated

Table 3
Validation conditions.

No.	Validation	Conditions	Exp.	Ref.
1	Thermal NO formation	2% H_2, 6% O_2, 92% N_2; initial temperature 2560 ± 50 K	Yes	[35]
2	Oxidation of HCN	318 ppm HCN, 1710 ppm CO, 2.4% O_2, 2.8% H_2O, balance N_2; temperature 900–1400 K	Yes	[36]
3	NO formation during conversion of coal-gasified fuel	5000 ppm O_2, 1000 ppm NO, 24 % CO, 9.1 % H_2, 1000 ppm NH_3, and balance N_2; temperature 873–1273 K	Yes	[33]
4	Oxidation of NH_3	2508/2513/2515 ppm CH_4, 3480/5040/40100 ppm (lean/stochiometric/rich) O_2, 484/468/468 ppm NH_3, balance N_2; temperature 973–1773 K	Yes	[21]
5	NO formation from the N_2O and NNH	17.4% CO, 82% air, 0.69–0.25% H_2 (decreasing with increasing temperature); temperature 1655–1725 K	Yes	[37]
6	Prompt NO formation	methane/air mixture (fuel–air equivalence ratio 0.68–1.54); temperature 1558–1979 K	Yes	[38]
7	SNCR with NH_3 (Thermal DeNOx)	832 ppm NH_3, 507 ppm NO, 4.0 % O_2, 10% H_2O, balance N_2; temperature 1050–1400 K	Yes	[39]
8	SNCR with cyanuric acid (RapReNOx)	470 ppm $(HOCN)_3$ (modeled as 1410 ppm HNCO), 330 ppm NO, 12.3 % O_2, 4.5 % H_2O, balance N_2; temperature 1100–1400 K	Yes	[40]
9	SNCR with urea (NOxout)	150 ppm urea (modeled as 150 ppm NH_3 and 150 ppm HNCO), 300 ppm NO, 4.0% O_2, 4.5% H_2O, balance N_2; temperature 1050–1350 K	Yes	[41]
10	NO formation during non-staged biomass combustion	excess air ratio* 0.6, 0.8, 1.0, 1.2, and 1.6; temperature 873–1673 K	No	
11	NO formation during staged biomass combustion	Air staging with two stages, 1st stage excess air ratio* 0.6 and 0.9, overall excess air ratio* 1.2 and 1.6; temperature (1st stage/2nd stage) 1073/1073, 1073/1273, 1173/1173, 1173/1373 K	No	
12	Effect of NO precursor speciation	HCN/NH_3 ratio 0.2, 0.5, 1.0, and 1.2; excess air ratio* 0.4, 0.6, 0.8, 1.0, 1.2, 1.4, and 1.6; temperature 1073 and 1673 K	No	

* Excess air ratio is defined based on the condition described in Section 2.3.

Table 4
Results from the necessity analysis.

Input species (I = 1)		Species	I	Species	I
Ar	O_2	H_2CN	1	H	0.4782
C_2H_4	C_2H_2	CH_3	0.9992	NNH	0.4219
CH_4	C_2H_6	NH_2	0.9979	CH_2O	0.4210
CO		C_2H_5	0.9971	HCCO	0.3554
CO_2		OH	0.9756	OCHO	0.3197
H_2		NO_2	0.9334	CH_2CHO	0.2800
H_2O		C_2H_3	0.8919	CH_3O	0.1910
HCN		CH_3OO	0.7102	H_2NO	0.1674
N_2		HCO	0.6220	CH_2	0.1546
NH_3		HO_2	0.6104	O	0.1274
NO		HNC	0.5717	CH_3CHN	0.1051

conditions, as shown in Fig. 2. The difference between results calculated using Glarborg148 and Li45 is almost negligible. In Fig. 2(a) for the oxidation of HCN, it is worth noting that the concentrations of HCN were unchanged in the simulations using Jepsen38 and Lovas36. This is primarily caused by the absence of the consumption channel HCN + OH = CN + H_2O in both mechanisms (R282, details can be found in the Supplemental material). Fig. 2(b) shows the conversion of NO and NH_3 during conversion of coal-gasified fuel. Since the condition is close to the reduction condition used to develop the skeletal mechanisms, very similar results were obtained. NO formation from N_2O and NNH is illustrated in Fig. 2(c). Due to the missing or incomplete NNH subset, the Jepsen38 and Lovas36 mechanisms cannot well predict the formation of NO. Fig. 2(d–f) shows the oxidation of NH_3 under three different conditions. Jepsen38 produced the poorest prediction, especially at high temperatures. It is difficult to attribute this to one single reason. The absence of the NNH subset in Jepsen38, however, might be the primary cause. Concentration profiles of OH and NO (in the v = 1 vibrational state) are shown in Fig. 2(g) for the validation of thermal NO formation. Owing to the missing N species and the corresponding reaction channels, Jepsen38 and Lovas36 failed to estimate the NO formation under the tested condition despite the accurate predictions of the concentration profile of OH. Since the important species such as NCN and CH are not included in Jepsen38 and Lovas36, it is no surprise that those two skeletal mechanisms cannot predict the prompt NO formation as shown in Fig. 2(h).

3.2. Further reduction

Despite around 70% reduction for both numbers of species and reactions reduced compared to the base mechanism, Li45 is still a relatively large kinetic set. A further reduction is needed to make the mechanism more suitable for large scale CFD simulations. As mentioned in the introduction, Jepsen38 is a very compact skeletal mechanism containing only 251 reactions. Thus, it was chosen as the basis for the further reduction. A few important species and reaction pathways presented in Li45, however, needed to be added into Jepsen38 to improve its predictability. This was achieved in several steps. First, species in Li45, Jepsen38, and Lovas36 were compared. Table 5 presents the shared species in all three skeletal mechanisms and the rest of the species in each individual mechanism.

All the shared species and reactions in Jepsen38 were retained in the new skeletal mechanism. Since it has been demonstrated that the Li45 mechanism has a very good predictability, species (C_2H, CH_2NH, CH_3CH_2O, H_2O_2, and He) and reactions that are not in Li45 were removed from Jepsen38. Secondly, the species N and its related reactions in Li45 were added to the new skeletal mechanism to address the issue related the thermal NO formation. Finally, a few reactions were added or modified (from non-reversible to reversible reaction using equilibrium estimations) to improve the predictability. The result is a skeletal mechanism that contains 32 species and 255 reactions (denoted as Li32). The complete mechanism in CHEMKIN format can be downloaded in the Supplemental material.

To be able to capture the SNCR processes, the Li32 mechanism was further modified. For the Thermal DeNOx process, one important intermediate species is the NNH, which provides a reaction path to convert NH_2 to N_2. It is, however, not included in Li32. A few reactions related to NNH were added to the new skeletal mechanism. Most of the reactions are related to the pathway of $NH_2 \rightarrow NNH \rightarrow N_2$. It should be noted that the inclusion of the reaction NNH + O = NH + NO (R243) improves the NO predictability at high temperatures by providing a NO formation channel from NNH. NO_2 has also been shown to be important in the Thermal DeNOx process [42–44], and thus needs to be added to the new mechanism. Since $NH_2 + NO_2 = H_2NO + NO$ (R222) is one of the main NO_2 consumption reactions, the subset of H_2NO was included accordingly. Another reaction between NH_2 and NO_2 ($NH_2 + NO_2 = N_2O + H_2O$, R223) was appended as well to make the NH_3 subset more complete. For the processes of RapReNOx and NOxout, HNCO (isocyanic acid) needs to be included as it is the decomposition product of both cyanuric acid and urea. The key reaction

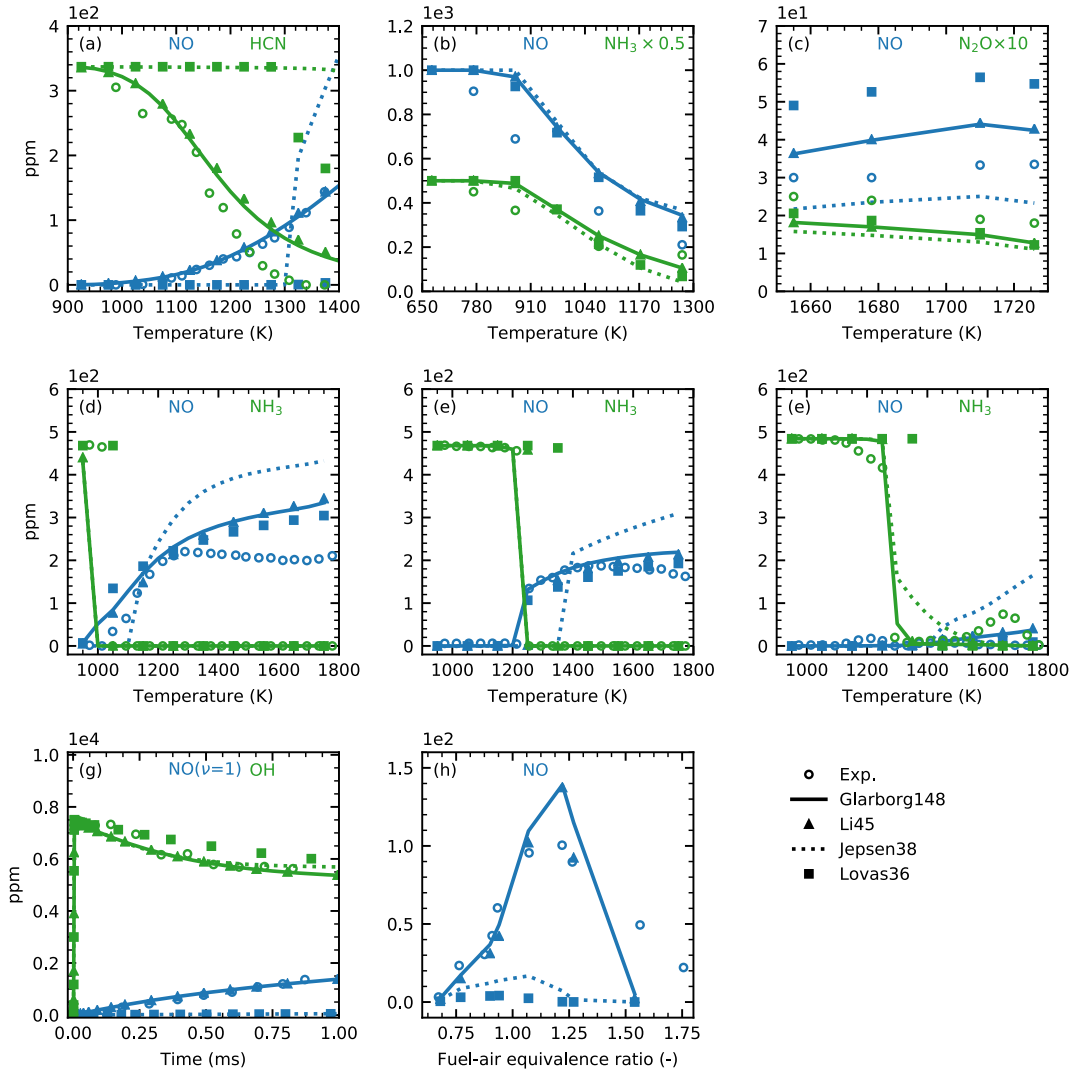

Fig. 2. Comparison between experiment and simulation under conditions of (a) oxidation of HCN, (b) NO formation during conversion of coal-gasified fuel, (c) NO formation from N_2O and NNH, (d) oxidation of NH_3 — lean condition, (e) oxidation of NH_3 — stoichiometric condition, (f) oxidation of NH_3 — rich condition, (g) thermal NO formation, (h) prompt NO formation.

for HNCO under oxidation conditions, HNCO + OH = NCO + H_2O (R307), was included. Moreover, the conversion paths between the HNCO and other species such HCN, HNC, and NH_2 were added to better connect the HNCO subset to the HCN and NH_3 subsets. The addition of HNC may further enhance the prediction of HCN oxidation as explained in a previous work [45]. After adding the above-mentioned species and reactions into Li32, a skeletal mechanism containing 37 species and 303 reactions was produced (denoted as Li37). The complete mechanism in CHEMKIN format can be found in the Supplemental material.

3.3. Analysis of the developed mechanisms

The underlying reaction flows in both Glarborg148 and Li37 were compared under the reduction condition (1073 K and an excess air ratio of 0.8). Figs. 3 and 4 display the element flowchart for nitrogen, with a filter size of minimum 20% of max flux for Glarborg148 and Li37, respectively. The arrow in the figure indicates the direction of the net flux, and its thickness corresponds to the magnitude of the net flux. We focused on the analysis of NO, N_2, and the two fuel nitrogen species NH_3 and HCN. As shown in Fig. 3 for the base Glarborg148 mechanism, NH_3 was first consumed to form the NH_2 radical, through primarily reaction with OH. HCN also partially converted to NH_2 via NCO and HNCO. The consumption of NH_2 led to four main different reaction flows of nitrogen: a formation of NO or N_2 via H_2NO and HNO, a direct conversion to N_2, a direct conversion to NH and subsequent to NO and N_2, and an indirect conversion to NH via a path consisting of amine, amino radicals, HCN, and NCO. The Li37 mechanism can reproduce most of the major conversion pathways as shown in Fig. 4. Due to the

Table 5
Species comparison between the different skeletal mechanisms.

	Jepsen38	Lovas36	Li45
Shared species	Ar C_2H_2 C_2H_3 C_2H_4 C_2H_5 C_2H_6 CH_2CHO CH_2O CH_3 CH_3O CH_4 CO CO_2 H H_2 H_2O HCN HCO HNO HO_2 N_2 N_2O NH NH_2 NH_3 NO O O_2 OH		
Individual species	CH CH_2 CH_3OO NCO C_2H CH_2NH CH_3CH_2O H_2O_2 He	CH_2CN CH_3CN H_2NO HCCO HNC NNH NO_2	CH CH_2 CH_3CHN CH_3OO CN H_2CN H_2NO HCCO HNC HNCO N NCN NCO NNH NO_2 OCHO

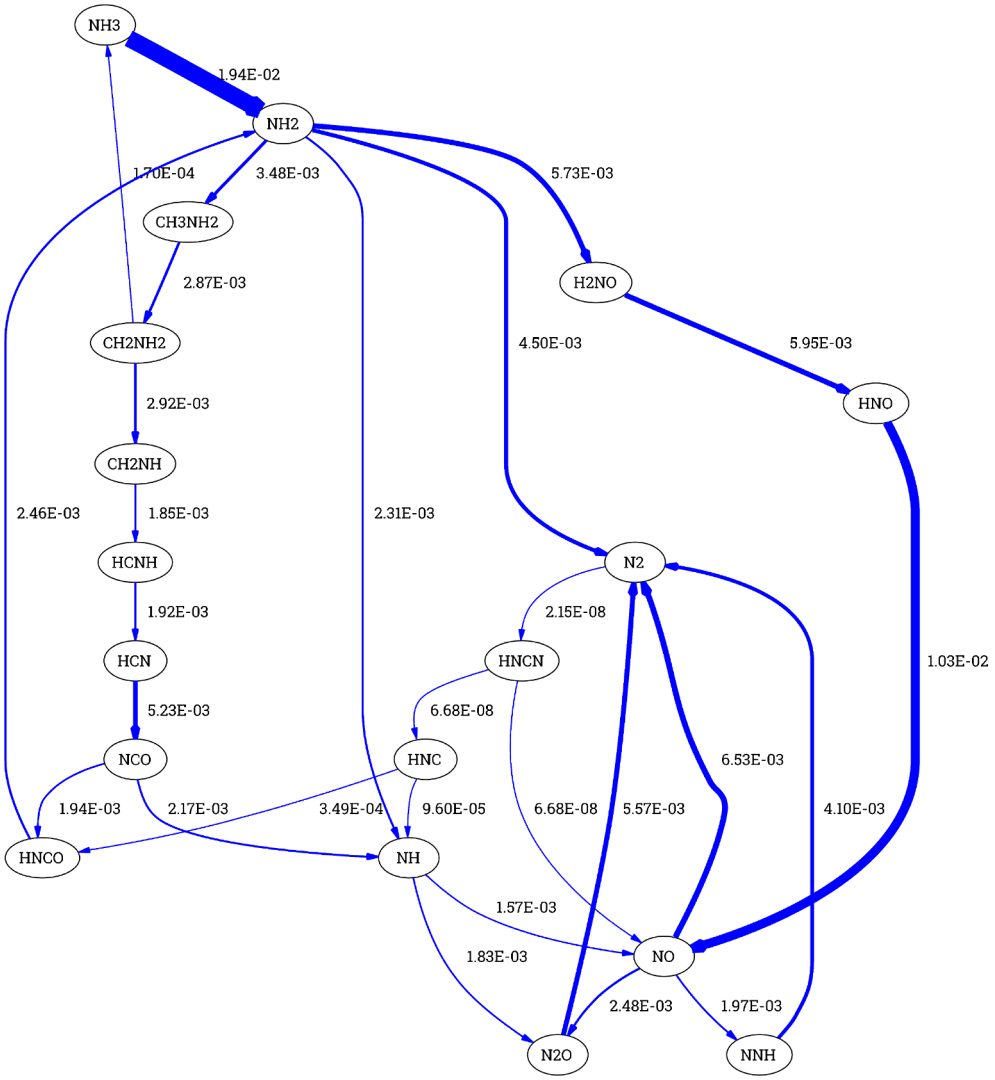

Fig. 3. Nitrogen flow chart at a temperature of 1073 K and an excess air ratio of 0.8 for Glarborg148, unit of the net flux is mol/m^3.

incomplete amino hydrocarbon subsets, Li37 contains one less consumption path for NH_2. It, however, has minor effects on the subsequent conversion paths NH→NO and NH→N_2O→N_2.

Figs. 5 and 6 show the element flowchart for nitrogen calculated at a temperature of 1373 K and an excess air ratio of 0.8 with the same filter size of 20% of max flux for Glarborg148 and Li37, respectively. Compared to Figs. 3 and 4, the reaction paths are much simpler at the higher temperature. Instead of converting mainly to H_2NO at the low temperature, NH_2 formed primarily NH at the elevated temperature. In the meantime, NH became also the main product of the NCO conversion. The formation paths of NO were also changed. The reaction path via NH and N became equally important as the path via HNO, which was well captured by Li37. The difference between Glarborg148 and Li37 at the high temperature may also result from the incomplete amino hydrocarbon related subsets. Again, its influence on formation of NO is insignificant. A large number of species and reactions are involved in those reaction pathways. In order to achieve a good computational efficiency, we decided not to include the complete amino hydrocarbon subsets.

3.4. Performance and applicability of the developed mechanisms

The three developed skeletal mechanisms were thoroughly compared to the detailed base kinetics under various conditions, including variations in temperature, excess air ratio, air staging configuration, and NO precursor speciation. Both Li45 and Li37 were also tested with regard to the predictability for SNCR processes. Comments on the applicability of the developed mechanisms for other combustion scenarios, as well as results related to the computational cost, are given at the end of this section.

3.4.1. Temperature and excess air ratio

Fig. 7 shows the detailed comparison between the different mechanisms on prediction of NO formation during combustion of biomass under various conditions as described in Table 3 (No. 10). When the temperature is lower than 1073 K as shown in Fig. 7(a and b), all the tested skeletal mechanisms have difficulties matching the NO profiles obtained using the base mechanism. The NO profiles calculated by Li32 deviated the most. This is mainly due to excluding NO_2 and the corresponding reactions, in particular NO + HO_2 = NO_2 + OH (R263) and NO_2 + H = NO + OH (R265). Those two reactions have very low activation energies, thus functioning even under low temperatures. The conversion between NO_2 and NO contributes significantly to the radical pool, which promotes the consumption of hydrogen and hydrocarbons. Such low temperature conditions, however, are of less importance in this study since the realistic furnaces usually operate at higher temperatures. At the temperature of 1073 K, all three developed skeletal mechanisms produced very similar NO profiles compared to the base

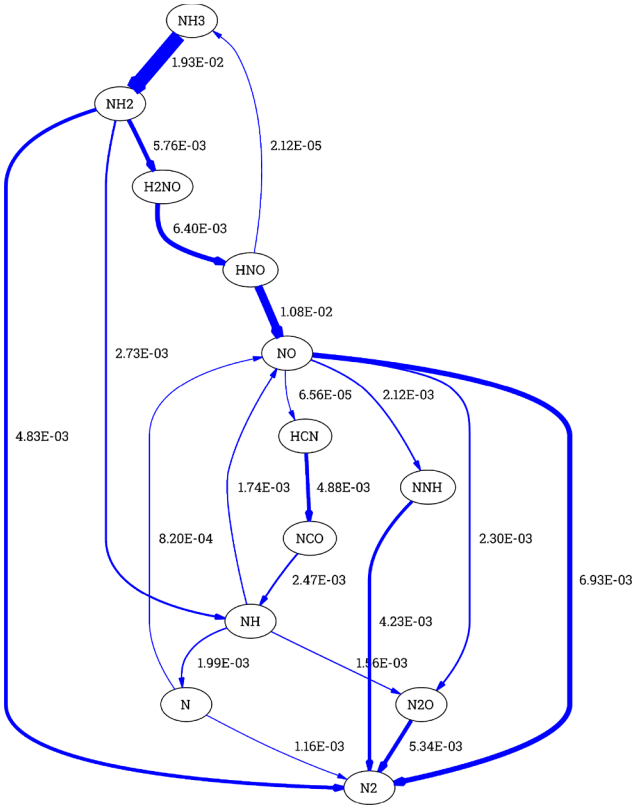

Fig. 4. Nitrogen flow chart at a temperature of 1073 K and an excess air ratio of 0.8 for Li37, unit of the net flux is mol/m^3.

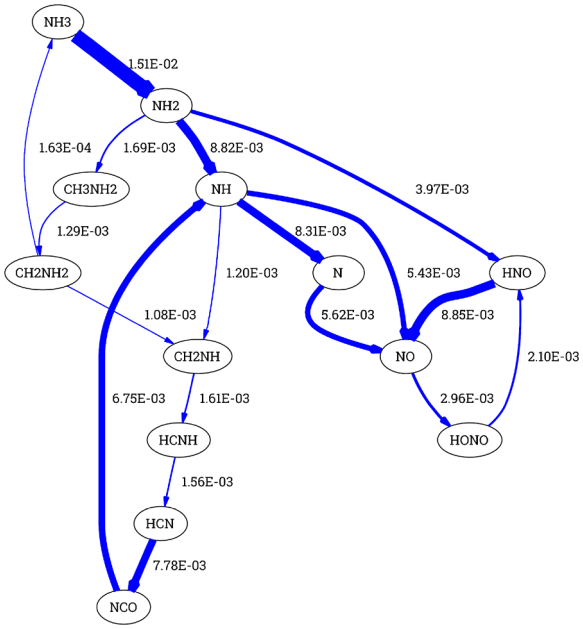

Fig. 5. Nitrogen flow chart at temperature of 1373 K and excess air ratio of 0.8 for Glarborg148, unit of the net flux is mol/m^3.

mechanism. A slight delay in predicting NO formation can be observed for Li32, particularly in the case with an excess air ratio of 0.8. This may also result from the exclusion of NO_2 containing reactions. At above 1073 K, all the skeletal mechanisms gave satisfactory results. Only a small difference can be found comparing with the fuel-rich cases having an excess air ratio of 0.6.

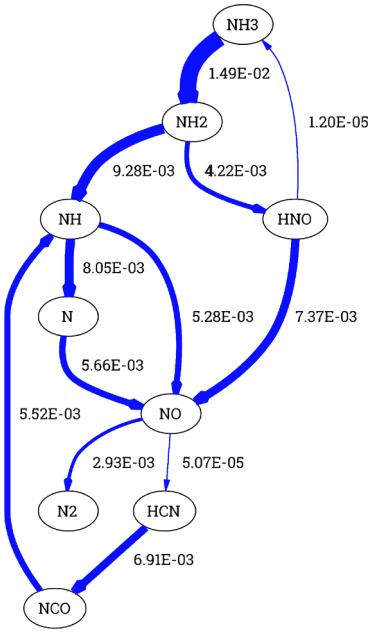

Fig. 6. Nitrogen flow chart at temperature of 1373 K and excess air ratio of 0.8 for Li37, unit of the net flux is mol/m^3.

3.4.2. Air staging combustion

As mentioned in the introduction, air staging combustion is a common technology to reduce NO_x formation. The performance of all developed skeletal mechanisms under several simulated air staging scenarios were investigated by comparing with the base mechanism. The detailed conditions are listed in Table 3 (No. 11). Two stages were included in simulations by two connected isothermal reactors. The obtained NO concentrations are shown in Fig. 8. When the temperature of the first stage is 1073 K, all the skeletal mechanisms in general agree well with the base mechanism. There are only two predictions obtained by Li32 having deviations lager than 20%. Those are the two conditions with both stages at 1073 K and an excess air ratio of 0.6 for the first stage, which are very challenging in kinetic modeling due to the complexity of the low temperature reaction paths at such a fuel rich condition. At higher first stage temperatures, all the skeletal mechanisms were able to estimate the NO concentration within 10% deviation compared to the base mechanism, thus demonstrating the excellent predictabilities under the tested air staging conditions.

3.4.3. NO precursor speciation

Apart from the temperature and excess air ratio, the NO precursor speciation can also be influential for NO formation during combustion of solid fuels [23]. The two most abundant NO precursors are HCN and NH_3. Therefore, simulations were configured with different ratios between HCN and NH_3 (from 0.2 to 1.2) to further examine the predictability of the skeletal mechanisms. As according to in Table 3 (No. 12), two temperatures (1073 and 1673 K) and excess air ratios ranging from 0.6 to 1.6 were used, which covers most of the typical operating conditions for grate-firing furnaces. The comparison between the base mechanism and all three skeletal mechanisms is illustrated in Fig. 9. The data points are colored depending on the ratio between HCN and NH_3. It is interesting to note that data points are grouped into clusters in Fig. 9. Those clusters in general have same temperature and excess air ratio. Therefore, the difference between the points in any given cluster is caused by the difference in the ratio between HCN and NH_3 as well as the choice of mechanism. Most of the data points lay along the diagonal line indicating predictions very close to the base mechanism, and none of them outside the 10 percentile, thus demonstrating the ability of the skeletal mechanisms to capture the effect of NO precursor

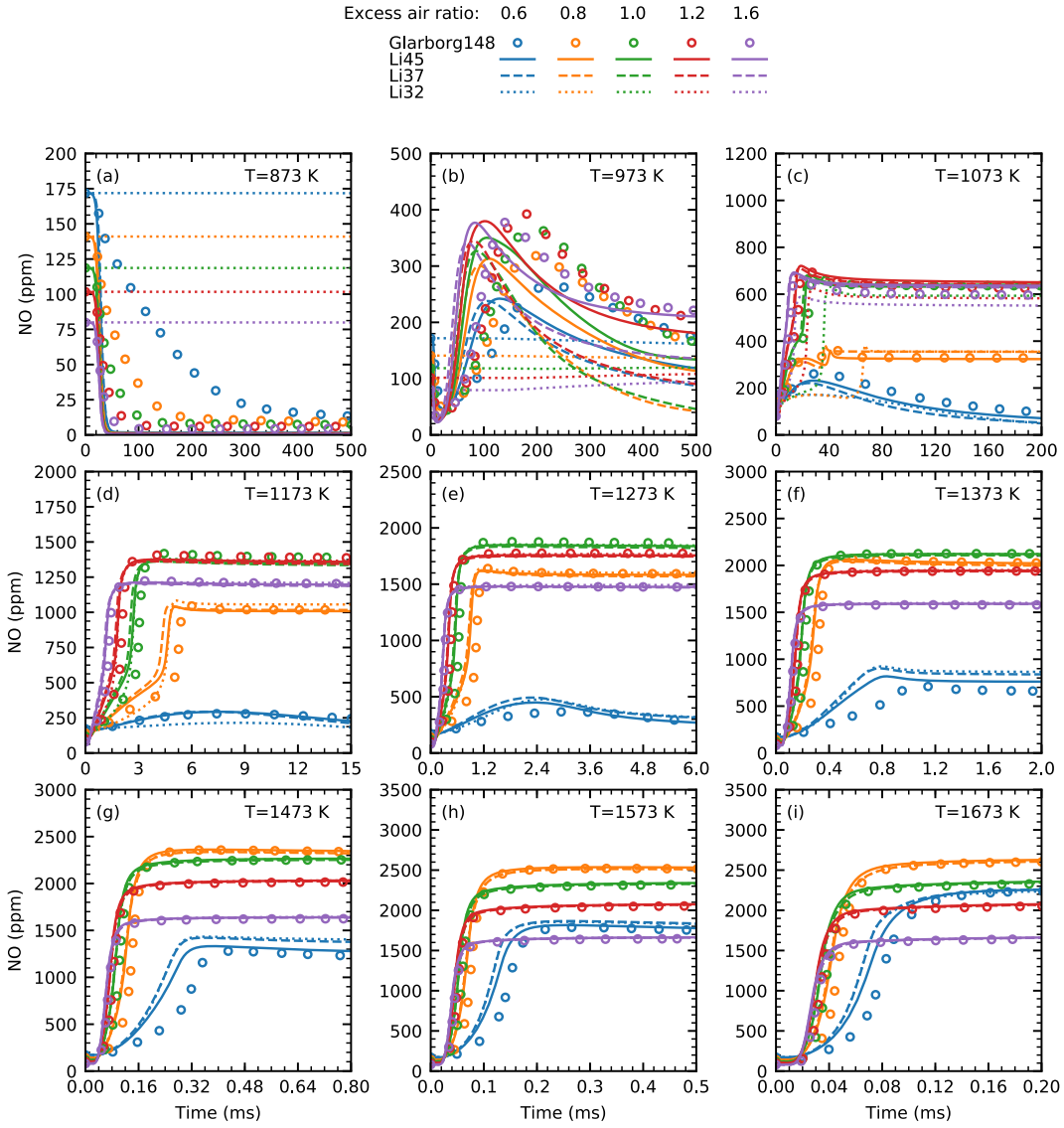

Fig. 7. Comparison between the skeletal mechanisms and Glarborg148 with regard to NO concentration profile with temperatures from 873 to 1673 K and excess air ratios from 0.6 to 1.6.

speciation on NO formation.

3.4.4. SNCR processes

To investigate the modeling capacity for SNCR, two skeletal mechanisms Li45 and Li37 were tested under conditions representing respectively three common SNCR technologies, Thermal DeNOx, RapReNOx, and NOxout, as detailed in Table 3 (No. 7–9). These conditions were chosen from previous experimental studies [39–41]. We intentionally selected the conditions with high concentration of H_2O and temperatures between 1000 and 1400 K to be close to the environment in the combustion chamber of grate-firing furnaces. Fig. 10 shows the comparison between experimental data and modeling results from Glarborg148, Li45, and Li37. All the kinetic models provided satisfactory predictions. A consistent underprediction of NO can be observed for Li37 at temperatures above 1300 K, but the deviations are relatively small. The reduction temperature window is an important parameter in design and operation of SNCR systems. As shown in Fig. 10, both Li45 and Li37 well captured the reduction temperature windows under all three representative SNCR conditions.

3.4.5. Applicability to other combustion technologies and fuels

Despite being developed under a condition close to biomass fired grate furnaces, the skeletal kinetic models have been thoroughly tested in a broad range of conditions against the base mechanism and experimental data. For suspension-firing furnaces, the operating temperature is typically higher than that in grate-firing furnaces. Based on the results shown in Fig. 7, it is clear that all three developed skeletal mechanisms are very capable of modeling NO conversion at high temperature conditions regardless of excess air ratio. Due to risk of ash sintering, relatively low operating temperature is required for fluidized-bed furnaces. However, temperatures over 1000 K can be expected in most of the scenarios [2]. Thus both suspension-firing and fluidized-bed furnaces can be relatively well modeled by the developed kinetics, especially Li45 and Li37. With regard to other types of fuels, for example coal and MSW, the main difference compared to biomass is the composition of the volatile gases. The formation of NO from fuel nitrogen, however, is predominantly affected by the speciation of the nitrogen containing species [23]. This has been extensively investigated. As a result, the developed kinetics in principle can also be applied to combustion of other solid fuels.

3.4.6. Computational cost

Fig. 11 shows a comparison between the different mechanisms regarding the computational cost. Simulations were configured similar to

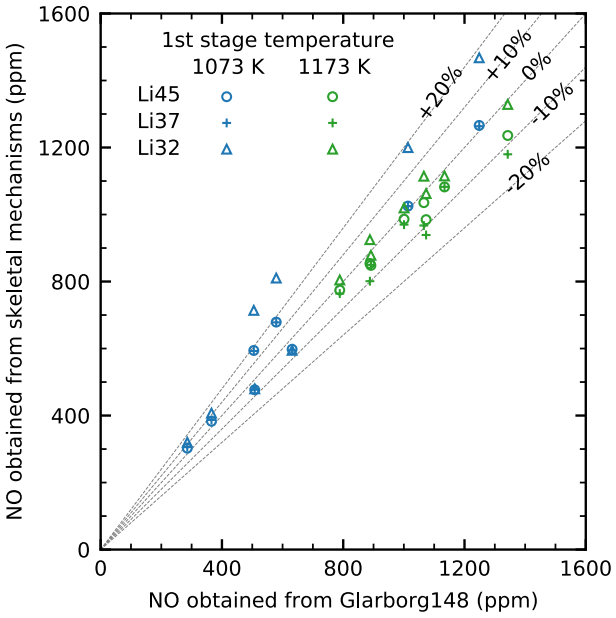

Fig. 8. Comparison between the skeletal mechanisms and Glarborg148 under air staging conditions.

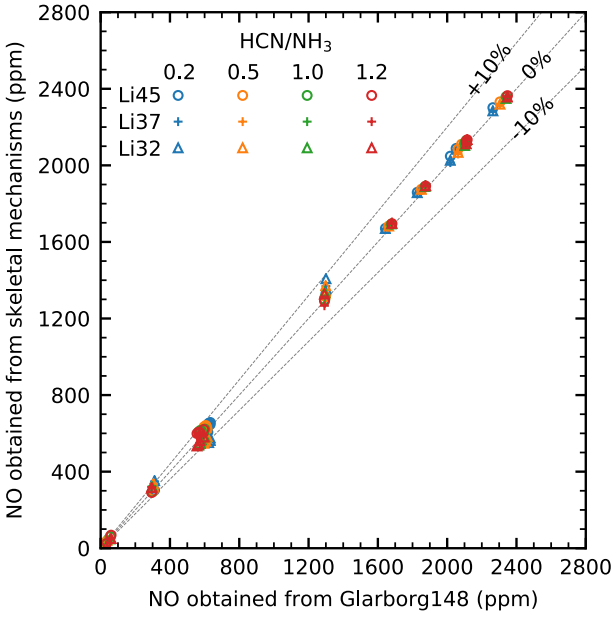

Fig. 9. Comparison between skeletal mechanisms and Glarborg148 with gas mixtures having different HCN and NH_3 ratios.

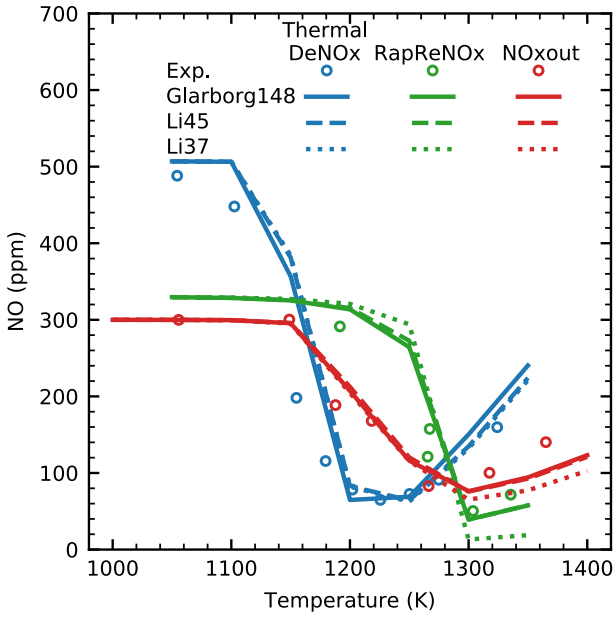

Fig. 10. Comparison between experimental data and modeling predictions under conditions similar to Thermal DeNOx [39], RapReNOx [40], and NOxout [41].

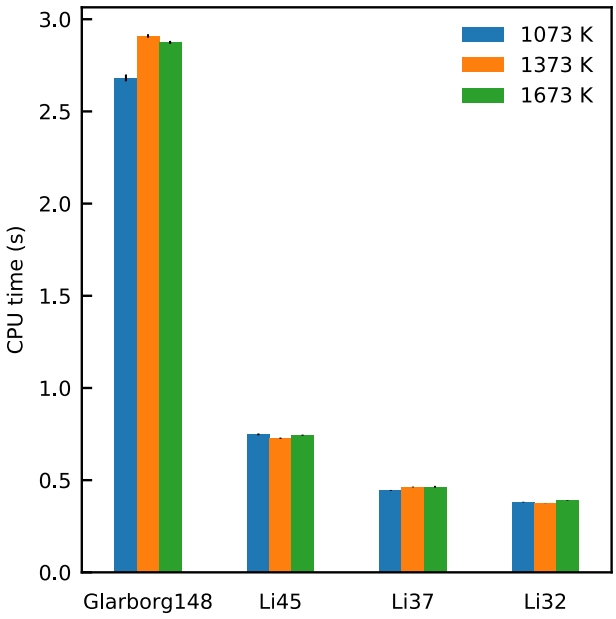

Fig. 11. Comparison of computational cost between different mechanisms at 1073, 1373 and 1673 K.

the setup described in Section 2.3 with the only exception of including two more temperatures: 1373 and 1673 K. The CPU time was obtained by averaging from three independent runs. The reduction in computational cost by the skeletal mechanisms are significant. Even with the largest skeletal set, Li45, around 73% CPU time reduction was achieved compared to the base mechanism. The Li37 and Li32 mechanisms, having less species and reactions, achieved around 84% and 86% reduction in computational cost, respectively. The results shown here reflect only the computational cost of the chemistry solver. Depending on the choice of the combustion model, there might be an additional cost in the CFD simulation related to solving the transport equation for each included species. Therefore, the cost of the CFD simulation may be heavily related to the total number of species in the kinetic mechanism. One may expect increased reduction in computational cost when using the skeletal mechanisms in CFD simulations.

4. Conclusion

Three skeletal mechanisms that are able to predict NO_x emission in solid fuel combustion were developed based on the comprehensive kinetic set proposed recently by Glarborg et al. [10]. Following the combined procedure of automatic necessity analysis and manual species addition, the resulted skeletal mechanism Li45 (45 species and 788 reactions) preserves the main reaction pathways of hydrocarbon conversion and NO formation, despite achieving around 70% reduction in number of species compared to the base mechanism. The comprehensive validation shows that Li45 is capable of reproducing experimental results under a broad range of conditions [21,33,35–41]. By comparing Li45 with the existing skeletal mechanisms [22,23] and through an in-depth analysis of the reaction pathways in the base mechanism under

relevant conditions, we proposed two additional skeletal mechanisms, Li32 (32 species and 255 reactions) and Li37 (37 species and 303 reactions).

All three skeletal mechanisms behaved very close to the base mechanism under most of the simulated conditions including variances in temperature, excess air ratio, air staging configuration, and NO precursor speciation. The largest deviation occurred when the reactor temperature is lower than 1073 K and at rather fuel rich conditions, which, however, happens rarely in realistic grate-firing furnaces. Li45 and Li37 have also been shown to well predict NO concentrations under conditions similar to common SNCR processes.

The computational cost of the three skeletal mechanisms were much lower than that of the detailed base mechanism, merely around 13% for the most compact Li32 mechanism. This together with having fewer species makes the developed mechanisms very attractive to be applied in large scale CFD simulations. Although the reduction is focused on predicting NO formation during combustion of biomass in grate-firing furnaces, the wide applicability range of the developed mechanisms should be suitable for simulating NO emission in other types of furnaces such as suspension-firing and fluidized-bed furnaces as well as in combustion of other solid fuels. The performance of the skeletal mechanisms in CFD simulations and in other combustion scenarios, however, requires further investigations.

Acknowledgments

The authors acknowledge the financial support by the Knowledge-Building Project GrateCFD (267957) funded by the Research Council of Norway and industry partners as well as the Researcher Project GASPRO (267916) funded by the Research Council of Norway.

Appendix A. Supplementary data

Supplementary data associated with this article can be found, in the online version, athttps://doi.org/10.1016/j.fuel.2019.05.152.

References

[1] The European Parliament, Directive (EU) 2015/2193 of the European Parliament and the Council of 25 November 2015; 2015.
[2] Loo SV, Koppejan J, editors. The Handbook of Biomass Combustion & Co-firing. London: Earthscan; 2008.
[3] Wendt JOL, Linak WP, Groff PW, Srivastava RK. Hybrid SNCR-SCR technologies for NO_x control: modeling and experiment. AIChE J. 2001;47(11):2603–17.
[4] Nussbaumer T. Combustion and co-combustion of biomass: fundamentals, technologies, and primary measures for emission reduction. Energy Fuels 2003;17(6):1510–21.
[5] Glarborg P, Jensen AD, Johnsson JE. Fuel nitrogen conversion in solid fuel fired systems. Prog. Energy Combust. Sci. 2003;29(2):89–113.
[6] Bowman CT. Control of combustion-generated nitrogen oxide emissions: technology driven by regulation. Symp. (Int.) Combust. 1992;24(1):859–78.
[7] Miller JA, Bowman CT. Mechanism and modeling of nitrogen chemistry in combustion. Prog. Energy Combust. Sci. 1989;15(4):287–338.
[8] Hill SC, Smoot LD. Modeling of nitrogen oxides formation and destruction in combustion systems. Prog. Energy Combust. Sci. 2000;26(4–6):417–58.
[9] Hayhurst AN, Vince IM. Nitric oxide formation from N2 in flames: The importance of “prompt” NO. Prog. Energy Combust. Sci. 1980;6(1):35–51.
[10] Glarborg P, Miller JA, Ruscic B, Klippenstein SJ. Modeling nitrogen chemistry in combustion. Prog. Energy Combust. Sci. 2018;67:31–68.
[11] Ruscic B, Pinzon RE, Morton ML, Laszevski GV, Bittner SJ, Nijsure SG, Amin KA, Minkoff M, Wagner AF. Introduction to active thermochemical tables: several “key” enthalpies of formation revisited. J. Phys. Chem. A 2004;108(45):9979–97.
[12] Ruscic B, Pinzon RE, Laszewski GV, Kodeboyina D, Burcat A, Leahy D, Montoy D, Wagner AF. Active thermochemical Tables: thermochemistry for the 21st century. J. Phys: Conf. Ser. 2005;16:561–70.
[13] Ranzi E, Frassoldati A, Grana R, Cuoci A, Faravelli T, Kelley AP, Law CK. Hierarchical and comparative kinetic modeling of laminar flame speeds of hydrocarbon and oxygenated fuels. Prog. Energy Combust. Sci. 2012;38(4):468–501.
[14] Faravelli T, Frassoldati A, Ranzi E. Kinetic modeling of the interactions between NO and hydrocarbons in the oxidation of hydrocarbons at low temperatures. Combust. Flame 2003;132(1–2):188–207.
[15] Frassoldati A, Faravelli T, Ranzi E. Kinetic modeling of the interactions between NO and hydrocarbons at high temperature. Combust. Flame 2003;135(1–2):97–112.
[16] Cuoci A, Frassoldati A, Faravelli T, Ranzi E. Formation of soot and nitrogen oxides in unsteady counterflow diffusion flames. Combust. Flame 2009;156(10):2010–22.
[17] Lu T, Law CK. Toward accommodating realistic fuel chemistry in large-scale computations. Prog. Energy Combust. Sci. 2009;35(2):192–215.
[18] Løvås T. Automatic generation of skeletal mechanisms for ignition combustion based on level of importance analysis. Combust. Flame 2009;156(7):1348–58.
[19] Lu T, Law CK. Systematic approach to obtain analytic solutions of quasi steady state species in reduced mechanisms. J. Phys. Chem. A 2006;110(49):13202–8.
[20] Houshfar E, Skreiberg Ø, Glarborg P, Løvås T. Reduced chemical kinetic mechanisms for NO_x emission prediction in biomass combustion. Int. J. Chem. Kinet. 2012;44(4):219–31.
[21] Mendiara T, Glarborg P. Ammonia chemistry in oxy-fuel combustion of methane. Combust. Flame 2009;156(10):1937–49.
[22] Løvås T, Houshfar E, Bugge M, Skreiberg Ø. Automatic generation of kinetic skeletal mechanisms for biomass combustion. Energy Fuels 2013;27(11):6979–91.
[23] Jepsen MS. NO reduction in grate-fired Waste-to-Energy plants. Technical University of Denmark; 2018. [Ph.D. thesis].
[24] Nagy T, Turányi T. Reduction of very large reaction mechanisms using methods based on simulation error minimization. Combust. Flame 2009;156(2):417–28.
[25] Han X, Wei X, Schnell U, Hein KRG. Detailed modeling of hybrid reburn/SNCR processes for NO_x reduction in coal-fired furnaces. Combust. Flame 2003;132(3):374–86.
[26] Lv Y, Wang Z, Zhou J, Cen K. Development and validation of a reduced mechanism for urea-based SNCR process based on QSS graph. Energy Fuels 2009;23(7):3605–11.
[27] Soyhan HS, Mauss F, Sorusbay C. Chemical kinetic modeling of combustion in internal combustion engines using reduced chemistry. Combust. Sci. Technol. 2002;174(11–12):73–91.
[28] Løvås T, Amnéus P, Mauss F, Mastorakos E. Comparison of automatic reduction procedures for ignition chemistry. Proc. Combust. Inst. 2002;29(1):1387–93.
[29] Houshfar E, Skreiberg Ø, Todorović D, Skreiberg A, Løvås T, Jović A, Sørum L. NO_x emission reduction by staged combustion in grate combustion of biomass fuels and fuel mixtures. Fuel 2012;98:29–40.
[30] Lyon RK. The NH3-NO-O2 reaction. Int. J. Chem. Kinet. 1976;8(2):315–8.
[31] Miller JA, Bowman CT. Kinetic modeling of the reduction of nitric oxide in combustion products by isocyanic acid. Int. J. Chem. Kinet. 1991;23(4):289–313.
[32] Muzio LJ, Arand JK, Teixeira DP. Gas phase decomposition of nitric oxide in combustion products. Symp. (Int.) Combust. 1977;16(1):199–208.
[33] Hasegawa T, Sato M. Study of ammonia removal from coal-gasified fuel. Combust. Flame 1998;114(1–2):246–58.
[34] LOGEresearch v1.10.0, LOGE AB; 2017.
[35] Bowman CT. Investigation of nitric oxide formation kinetics in combustion processes: the hydrogen-oxygen-nitrogen reaction. Combust. Sci. Technol. 1971;3(1):37–45.
[36] Glarborg P, Miller JA. Mechanism and modeling of hydrogen-cyanide oxidation in a flow reactor. Combust. Flame 1994;99(3–4):475–83.
[37] Steele RC, Malte PC, Nicol DG, Kramlich JC. NO_x and N2O in lean-premixed jet-stirred flames. Combust. Flame 1995;100(3):440–9.
[38] Bartok W, Engleman VS, Goldstein R, Del Valle EG. Basic kinetic studies and modeling of nitrogen oxide formation in combustion progresses. AIChE Symp. 1972;68(126):30–8.
[39] Duo W. Kinetic studies of the reactions involved in selective non-catalytic reduction of nitric oxide. Technical University of Denmark; 1990. [Ph.D. thesis].
[40] Caton JA, Siebers DL. Comparison of nitric oxide removal by cyanuric acid and by ammonia. Combust. Sci. Technol. 1989;65(4–6):277–93.
[41] Alzueta MU, Røjel H, Kristensen PG, Glarborg P, Dam-Johansen K. Laboratory study of the CO/NH3/NO/O2 system: implications for hybrid reburn/SNCR strategies. Energy Fuels 1997;11(3):716–23.
[42] Miller JA, Glarborg P. Modeling the thermal De-NO_x process: closing in on a final solution. Int. J. Chem. Kinet. 1999;31(11):757–65.
[43] Miller JA, Glarborg P. Modelling the formation of N_2O and NO_2 in the thermal De-NO_x process. In: Wolfrum J, Volpp H, Rannacher R, Warnatz J, editors. Gas phase chemical reaction systems. Springer; 1996. p. 318–33.
[44] Klippenstein SJ, Harding LB, Glarborg P, Miller JA. The role of NNH in NO formation and control. Combust. Flame 2011;158(4):774–89.
[45] Lin MC, He Y, Melius CF. Implications of the HCN→HNC process to high-temperature nitrogen-containing fuel chemistry. Int. J. Chem. Kinet. 1992;24(12):1103–7.